

Low-Density Spin Susceptibility and Effective Mass of Mobile Electrons in Si Inversion Layers

V. M. Pudalov,^{1,2} M. E. Gershenson,¹ H. Kojima,¹ N. Butch,¹ E. M. Dizhur,³ G. Brunthaler,⁴ A. Prinz,⁴ and G. Bauer⁴

¹*Department of Physics and Astronomy, Rutgers University, Piscataway, New Jersey 08854*

²*P. N. Lebedev Physics Institute, 119991 Moscow, Russia*

³*Institute for High Pressure Physics, Troitsk, Russia*

⁴*Institut für Halbleiterphysik, Johannes Kepler Universität, Linz, Austria*

(Received 9 October 2001; published 30 April 2002)

We studied the Shubnikov–de Haas (SdH) oscillations in high-mobility Si-MOS samples over a wide range of carrier densities $n \approx (1-50) \times 10^{11} \text{ cm}^{-2}$, which includes the vicinity of the apparent metal-insulator transition in two dimensions (2D MIT). Using a novel technique of measuring the SdH oscillations in superimposed and independently controlled parallel and perpendicular magnetic fields, we determined the spin susceptibility χ^* , the effective mass m^* , and the g^* factor for mobile electrons. These quantities increase gradually with decreasing density; near the 2D MIT, we observed enhancement of χ^* by a factor of ~ 4.7 .

DOI: 10.1103/PhysRevLett.88.196404

PACS numbers: 71.30.+h, 71.27.+a, 73.40.Qv

Many two-dimensional (2D) systems exhibit an apparent metal-insulator transition (MIT) at low temperatures as the electron density n is decreased below a critical density n_c (for reviews, see, e.g., Refs. [1–3]). The phenomena of the MIT and “metallic” conductivity in 2D attract a great deal of interest, because it addresses a fundamental problem of the ground state of strongly correlated electron systems. The strength of electron-electron interactions is characterized by the ratio r_s of the Coulomb interaction energy to the Fermi energy ϵ_F . The 2D MIT is observed in Si MOSFETs at $n_c \sim 1 \times 10^{11} \text{ cm}^{-2}$, which corresponds to $r_s \sim 8$ [for 2D electrons in (100)-Si, $r_s = 2.63\sqrt{10^{12} \text{ cm}^{-2}/n}$].

In the theory of electron liquid, the electron effective mass m^* , the g^* factor, and the spin susceptibility $\chi^* \propto g^* m^*$ are renormalized depending on r_s [4]. Though the quantitative theoretical results [5–7] vary considerably, all of them suggest enhancement of χ^* , m^* , and g^* with r_s . Earlier experiments [8–11] have shown growth of m^* and $g^* m^*$ at relatively small r_s values, pointing to a ferromagnetic type of interactions in the explored range $1 \lesssim r_s < 6.5$. Potentially, strong interactions might drive an electron system towards ferromagnetic instability [4]. Moreover, it has been suggested that the metallic behavior in 2D is accompanied by a tendency to a ferromagnetic instability [12]. Thus, in relation to the still open question of the origin of the 2D MIT, direct measurements of these quantities in the dilute regime near the 2D MIT are crucial.

In this Letter, we report the *direct* measurements of χ^* , m^* , and, hence, g^* over a wide range of carrier densities ($1 \leq r_s \leq 8.4$), which extends for the first time down to and across the 2D MIT. The data were obtained by a novel technique of measuring the interference pattern of Shubnikov–de Haas (SdH) oscillations in *crossed magnetic fields*. The conventional technique of measuring $g^* m^*$ in tilted magnetic fields [8,10] is not applicable when the Zeeman energy is greater than half the cyclotron energy [13]. The crossed field technique removes this restric-

tion and allows us to extend measurements over the wider range of r_s . We find that, for small r_s , the $g^* m^*$ values increase slowly in agreement with the earlier data by Fang and Stiles [8] and Okamoto *et al.* [10]. For larger values of r_s , $g^* m^*$ grows faster than it might be extrapolated from the earlier data. At our highest value of $r_s \approx 8.4$, the measured $g^* m^*$ is greater by a factor of 4.7 than that at low r_s .

Our resistivity measurements were performed by ac (13 Hz) technique at the bath temperatures 0.05–1.6 K, on seven (100) Si-MOS samples selected from four wafers: Si12 (peak mobility $\mu \approx 3.4 \text{ m}^2/\text{Vs}$ at $T = 0.3 \text{ K}$), Si22 ($\mu \approx 3.2 \text{ m}^2/\text{Vs}$), Si57, Si3-10, Si6-14/5, Si6-14/10, and Si6-14/18 ($\mu \approx 2.4 \text{ m}^2/\text{Vs}$ for the latter five samples) [14]. The gate oxide thickness was $190 \pm 20 \text{ nm}$ for all the samples; the 2D channel was oriented along [011] for sample Si3-10, for all other samples—along [010]. The crossed magnetic field system consists of two magnets, whose fields can be varied independently. A split coil, producing the field $B_\perp \leq 1.5 \text{ T}$ normal to the plane of the 2D layer, is positioned inside the main solenoid, which creates the in-plane field B_\parallel up to 8 T. The electron density was determined from the period of SdH oscillations.

Typical traces of the longitudinal resistivity ρ_{xx} as a function of B_\perp are shown in Fig. 1. Because of the high electron mobility, oscillations were detectable down to 0.25 T, and a large number of oscillations enabled us to extract the fitting parameters $g^* m^*$ and m^* with a high accuracy. The oscillatory component $\delta\rho_{xx}$ was obtained by subtracting the monotonic “background” magnetoresistance (MR) from the $\rho_{xx}(B_\perp)$ dependence (the background MR is more pronounced for lower n ; compare Figs. 1 and 3).

The theoretical expression for the oscillatory component of the magnetoresistance is as follows [15]:

$$\frac{\delta\rho_{xx}}{\rho_0} = \sum_s A_s \cos\left[\pi s \left(\frac{\hbar\pi n}{eB_\perp} - 1\right)\right] Z_s, \quad (1)$$

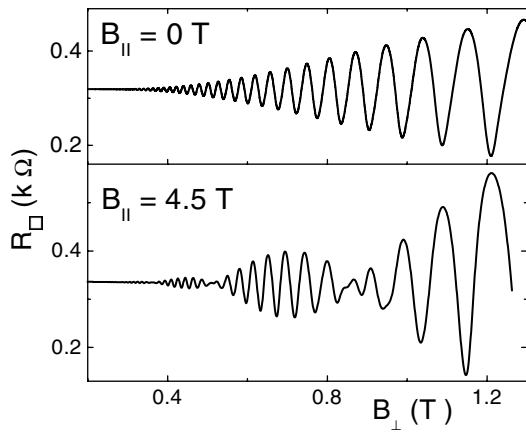


FIG. 1. Shubnikov-de Haas oscillations for $n = 10.6 \times 10^{11} \text{ cm}^{-2}$ (sample Si6-14/10) at $T = 0.35 \text{ K}$.

where

$$A_s = 4 \exp\left(-2\pi^2 s \frac{k_B T_D}{\hbar \omega_c}\right) \frac{2\pi^2 s k_B T / \hbar \omega_c}{\sinh(2\pi^2 s k_B T / \hbar \omega_c)}. \quad (2)$$

Here $\rho_0 = \rho_{xx}(B_{\perp} = 0)$, $\omega_c = eB_{\perp}/m^*m_e$ is the cyclotron frequency, m^* is the dimensionless effective mass, m_e is the free electron mass, and T_D is the Dingle temperature. We take the valley degeneracy $g_v = 2$ in Eqs. (1) and (2) and throughout the paper. The Zeeman term $Z_s = \cos[\pi s \hbar \pi (n_{\uparrow} - n_{\downarrow}) / (eB_{\perp})]$ reduces to a field-independent constant for $B_{\parallel} = 0$.

Application of B_{\parallel} induces beating of SdH oscillations, which are observed as a function of B_{\perp} . The beat frequency is proportional to the spin polarization of the interacting 2D electron system [16]:

$$P \equiv \frac{n_{\uparrow} - n_{\downarrow}}{n} = \frac{\chi^* B_{\text{tot}}}{g_b \mu_B n} = g^* m^* \frac{e B_{\text{tot}}}{nh}, \quad (3)$$

where n_{\uparrow} (n_{\downarrow}) stands for the density of spin-up (spin-down) electrons, $g_b \approx 2$ is the bare g factor for Si, and $B_{\text{tot}} = \sqrt{B_{\perp}^2 + B_{\parallel}^2}$. Equations (2) and (3) imply that the spin polarization of the electron system is linear in B_{tot} (relevance of this assumption to our experiment will be justified below).

In the experiment, we observed a well-pronounced beating pattern at a nonzero B_{\parallel} (Figs. 1 and 2), in agreement with Eq. (1). The phase of SdH oscillations remains the same between the adjacent beating nodes, and changes by π through the node. The interference pattern (including positions of the nodes) is controlled by Z_s in Eq. (1) and is defined solely by g^*m^* . Systematic study of this pattern enables us to determine g^*m^* with high accuracy ($\sim 2\%$ – 5%). The g^*m^* values are independent of T (at $T < 1 \text{ K}$) within our accuracy. We have observed a B_{\parallel} dependence of g^*m^* in strong parallel fields; it is more pronounced near the 2D MIT, where g^*m^* varies with B_{\parallel} by $\sim 15\%$. To determine g^*m^* in the linear regime, we systematically measured, for each n , the beating pattern at decreasing values of B_{\parallel} until g^*m^* becomes indepen-

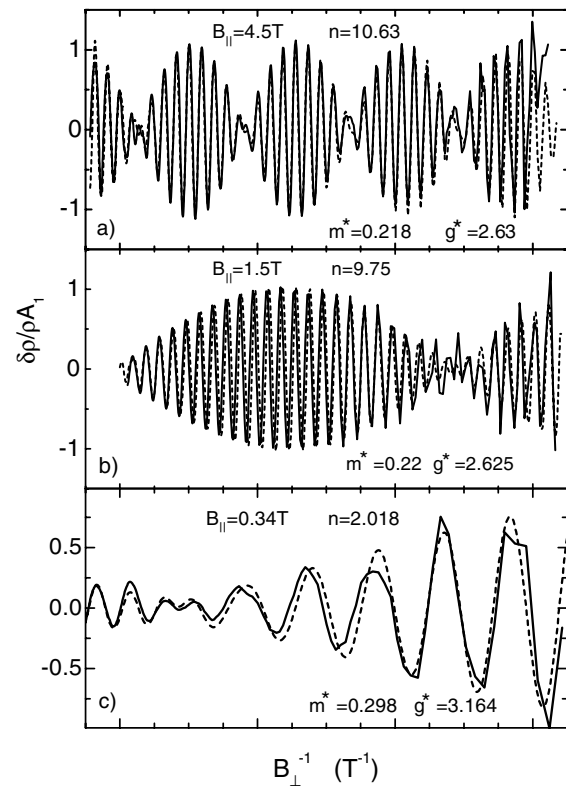


FIG. 2. Examples of fitting with Eq. (1): (a) $n = 10.6 \times 10^{11} \text{ cm}^{-2}$, $T = 0.35 \text{ K}$, $B_{\parallel} = 4.5 \text{ T}$ (the data correspond to Fig. 1); (b) $n = 9.75 \times 10^{11} \text{ cm}^{-2}$, $B_{\parallel} = 1.5 \text{ T}$; (c) $n = 2.02 \times 10^{11} \text{ cm}^{-2}$, $T = 0.2 \text{ K}$, $B_{\parallel} = 0.34 \text{ T}$. The data for sample Si6-14/10 are shown as the solid lines, the fits (with parameters shown) as dashed lines. All are normalized by $A_1(B_{\perp})$.

dent of B_{\parallel} . Typically, the linear regime corresponded to $B_{\parallel} \sim 1 \text{ T}$ at high densities, $n \sim 10^{12} \text{ cm}^{-2}$, and to $B_{\parallel} \approx 0.1$ – 0.4 T at low densities, $n \sim 10^{11} \text{ cm}^{-2}$.

Comparison between the measured and calculated dependences $\delta\rho_{xx}/\rho_0$ versus B_{\perp} , both normalized by the amplitude of the first harmonic A_1 , is shown in Fig. 2 for three carrier densities. The normalization assigns equal weights to all oscillations. We analyzed SdH oscillations over the low-field range $B_{\perp} \leq 1 \text{ T}$; this limitation arises from the assumption in Eq. (1) that $\hbar\omega_c \ll \epsilon_F$ and $\delta\rho_{xx}/\rho_0 \ll 1$. The latter condition also allows us to neglect the interlevel interaction which is known to enhance g^* in stronger fields [18].

The amplitude of SdH oscillations at small B_{\perp} can be significantly enhanced by applying B_{\parallel} (see Fig. 3), which is another advantage of the cross-field technique. Indeed, for low B_{\perp} and n , the electron energy spectrum is complicated by crossing of levels corresponding to different spins/valleys. By applying B_{\parallel} , we can control the energy separation between the levels, and enhance the amplitude of low- B oscillations (see Fig. 3). We have verified that application of B_{\parallel} (up to the spin polarization $\sim 20\%$) does not affect the extracted m^* values (within 10% accuracy), provided the sample remains in the metallic regime (the

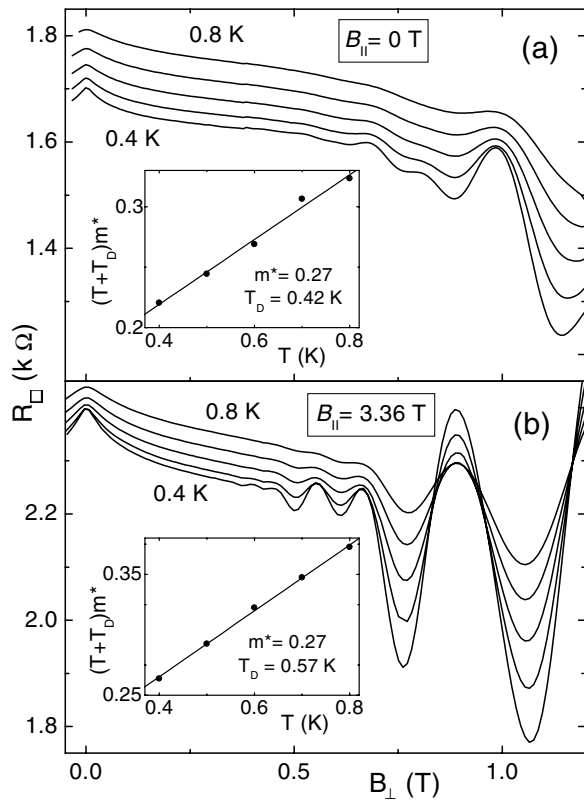


FIG. 3. Shubnikov-de Haas oscillations versus B_{\perp} for sample Si6-14/10 ($n = 2.2 \times 10^{11} \text{ cm}^{-2}$) at $T = 0.4, 0.5, 0.6, 0.7,$ and 0.8 K : (a) $B_{\parallel} = 0$ and (b) $B_{\parallel} = 3.36 \text{ T}$. The insets show the temperature dependences of fitting parameters $(T + T_D)m^*$.

insets of Fig. 3 show that the values of m^* measured at $B_{\parallel} = 0$ and 3.36 T do coincide).

Fitting of the data provides us with two combinations of parameters: g^*m^* and $(T + T_D)m^*$. The measured values of g^*m^* , as well as m^* which are discussed below, were similar for different samples. Figure 4a shows that, for small r_s , our g^*m^* values agree with the earlier data by Fang and Stiles [8] and Okamoto *et al.* [10]. For $r_s \geq 6$, g^*m^* increases with r_s faster than it might be expected from extrapolation of the earlier results [10]. The MIT occurs at the critical r_s value ranging from $r_c = 7.9$ to 8.8 for different samples; in particular, $r_c \approx 8.2$ for samples Si6-14/5, 10, 18 which have been studied down to the MIT.

An interesting question is whether the measured dependence $\chi^*(r_s)$ shown in Fig. 4a represents a critical behavior as might be expected if χ^* diverges at n_c . Analysis of the B_{\parallel} -induced magnetoresistance led the authors of Refs. [20,21] to the conclusion that there is a ferromagnetic instability at $n \approx n_c$. Our results, which do not support the occurrence of spontaneous spin polarization and divergence of χ^* at $n = n_c$, are presented in Ref. [17].

The second combination, $(T + T_D)m^*$, controls the amplitude of oscillations. In order to disentangle T_D and m^* , we analyzed the temperature dependence of oscillations over the range $T = 0.3\text{--}1.6 \text{ K}$ (for some samples $0.4\text{--}0.8 \text{ K}$) [19]. The conventional procedure of calculat-

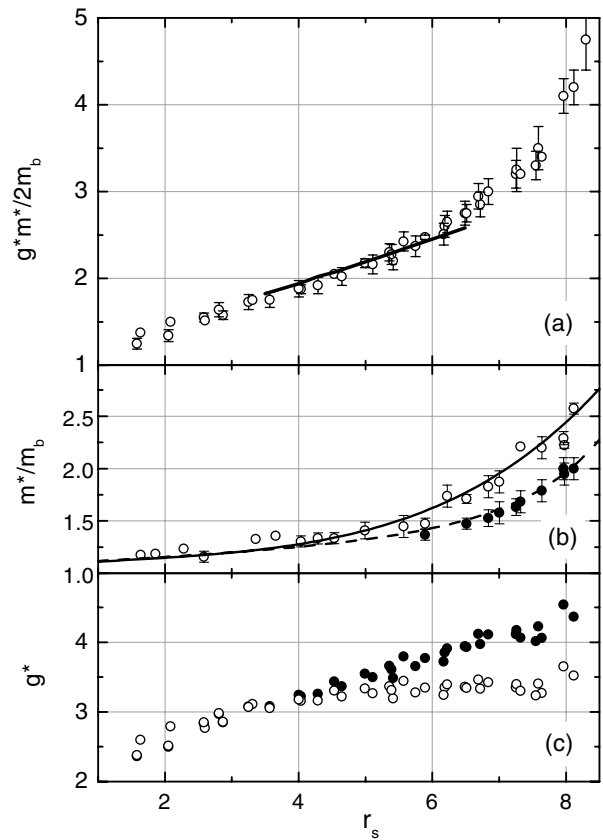


FIG. 4. Parameters g^*m^* , m^* , and g^* for different samples as a function of r_s (dots). The solid line in (a) shows the data by Okamoto *et al.* [10]. The solid and open dots in (b) and (c) correspond to two different methods of finding m^* (see the text). The solid line and the dashed line in (b) are polynomial fits for the two dependences $m^*(r_s)$. The values of g^* shown in (c) were obtained by dividing the g^*m^* data by the smooth approximations of the experimental dependences $m^*(r_s)$ shown in (b).

ing the effective mass for low r_s values (≤ 5), based on the assumption that T_D is T independent, is illustrated by the insets of Fig. 3. In this small- r_s range, our results are in good agreement with the earlier data by Smith and Stiles [9], and by Pan *et al.* [11]. The assumption $T_D \neq f(T)$, however, becomes dubious near the MIT, where the resistance varies significantly over the studied temperature range; in this case, the two parameters T_D and m^* become progressively more correlated. The open dots in Fig. 4b were obtained by assuming that T_D is T independent over the whole explored range of n : m^* increases with r_s , and the ratio m^*/m_b becomes ~ 2.5 at $r_s = 8$ ($m_b = 0.19$ is the band mass). As another limiting case, one can attribute the change in $R(T)$ solely to the temperature dependence of the short-range scattering and request T_D to be proportional to $R(T)$. In the latter case, the extracted dependence $m^*(r_s)$ is weaker (the solid dots in Fig. 4b). To reduce the uncertainty of m^* at large r_s , it is necessary to separate the effects of T -dependent scattering and “smearing” of the Fermi distribution in the dependence $R(T)$; an adequate theory is currently unavailable.

Our data shows that the combination $(T + T_D)m^*$ is almost the same for electrons in both spin-up and spin-down subbands [e.g., for $n = 3.76 \times 10^{11} \text{ cm}^{-2}$ and $B_{\parallel} = 2.15 \text{ T}$ ($P = 20\%$), the T_D values for “spin-up” and “spin-down” levels differ by $\leq 3\%$]. This is demonstrated by the observed almost 100% modulation of SdH oscillations (see, e.g., Figs. 2a and 2b). Thus, the carriers in the spin-up and spin-down subbands have nearly the same mobility; this imposes some constraints on theoretical models of electron transport in the 2D metallic state.

In conclusion, using a novel cross-field technique for measuring SdH oscillations, we performed direct measurements of the spin susceptibility, effective mass, and g factor of conducting electrons over a wide range of carrier densities. By studying the temperature dependence of SdH oscillations, we disentangled three unknown parameters (g^* , m^* , and T_D) and obtained their values in the limit of small magnetic fields. We found that both g^*m^* and m^* are almost independent of the temperature over the range 0.3–1 K. At the 2D metal-insulator transition, we observed a finite value of the spin susceptibility, enhanced by a factor of ~ 4.7 with respect to the high-density limit.

The authors are grateful to E. Abrahams, I. Aleiner, B. Altshuler, and D. Maslov for discussions. The work was supported by the NSF, ARO MURI, NATO Scientific Program, RFBR, FWF, INTAS, and the Russian Programs “Physics of Nanostructures,” “Quantum Non-Linear Processes,” “Integration,” “Physics of Quantum Computing and Telecommunications,” and “The State Support of Leading Scientific Schools.”

-
- [1] E. Abrahams, S. V. Kravchenko, and M. P. Sarachik, *Rev. Mod. Phys.* **73**, 251 (2001).
 - [2] B. L. Altshuler, D. L. Maslov, and V. M. Pudalov, *Physica (Amsterdam)* **9E**, 209 (2001).
 - [3] V. M. Pudalov, G. Brunthaler, A. Prinz, and G. Bauer, *cond-mat/0103087*.
 - [4] A. A. Abrikosov, *Fundamentals of the Theory of Metals* (North-Holland, Amsterdam, 1988); A. Isihara, *Electron Liquids* (Springer-Verlag, Berlin, 1997).

- [5] N. Iwamoto, *Phys. Rev. B* **43**, 2174 (1991).
- [6] Y. Kwon, D. M. Ceperley, and R. M. Martin, *Phys. Rev. B* **50**, 1684 (1994).
- [7] G.-H. Chen and M. E. Raikh, *Phys. Rev. B* **60**, 4826 (1999).
- [8] F. F. Fang and P. J. Stiles, *Phys. Rev. B* **174**, 823 (1968).
- [9] J. L. Smith and P. J. Stiles, *Phys. Rev. Lett.* **29**, 102 (1972).
- [10] T. Okamoto, K. Hosoya, S. Kawaji, and A. Yagi, *Phys. Rev. Lett.* **82**, 3875 (1999).
- [11] W. Pan, D. C. Tsui, and B. L. Draper, *Phys. Rev. B* **59**, 10 208 (1999).
- [12] A. M. Finkel'stein, *Z. Phys. Cond. Matter* **56**, 189 (1984); *Sov. Sci. Rev. A, Phys. Rev.* **14**, 1 (1990); C. Castellani, C. DiCastro, P. A. Lee, M. Ma, S. Sorella, and E. Tabet, *Phys. Rev. B* **30**, 1596 (1984).
- [13] The common technique of measuring g^*m^* in a tilted field is based on detecting the disappearance of the first harmonic of oscillations when $2g^*\mu_B B_{\text{tot}} = \hbar e B_{\perp} / (m^* m_e)$. This technique is applicable only up to $r_s = 6.3$ [10].
- [14] Samples Si6-14/5, 10, 18 correspond to the same chip Si6-14 cooled from 300 down to 4.2 K, while holding the gate voltage V_g at 5, 10, and 18 V. These “samples” showed different parallel-field MR at low T .
- [15] I. M. Lifshitz and A. M. Kosevich, *Zh. Eksp. Teor. Fiz.* **29**, 730 (1955); A. Isihara and L. Smrčka, *J. Phys. C* **19**, 6777 (1986).
- [16] Yu. A. Bychkov and L. P. Gor'kov, *Sov. Phys. JETP* **14**, 1132 (1982).
- [17] V. M. Pudalov, M. E. Gershenson, and H. Kojima, *cond-mat/0110160*.
- [18] The oscillatory behavior of the g^* factor in high B_{\perp} is related to the exchange interaction between Landau levels (see, e.g., Isihara [4]). This interaction leads to the enhancement of the g^* value averaged over the period of oscillations [for the Si data, see V. M. Pudalov *et al.*, *J. Exp. Theor. Phys.* **62**, 1079 (1985)]. In low fields and the weak SdH effect regime, the interlevel interaction can be ignored.
- [19] Below 0.3 K, we observed the trend of simultaneous saturation of the temperature dependences of ρ_0 , $\delta\rho_{xx}$, and the dephasing rate, which is presumably caused by electron overheating.
- [20] A. A. Shashkin, S. V. Kravchenko, V. T. Dolgoplov, and T. M. Klapwijk, *Phys. Rev. Lett.* **87**, 086801 (2001).
- [21] S. A. Vitkalov, H. Zheng, K. M. Mertes, M. P. Sarachik, and T. M. Klapwijk, *Phys. Rev. Lett.* **87**, 086401 (2001).